ADVANCED MATERIALS
www.advmat.de

Schottky-Contacted Nanowire Sensors

*Jianping Meng and Zhou Li**

The progress of the Internet-of-Things in the past few years has necessitated the support of high-performance sensors. Schottky-contacted nanowire sensors have attracted considerable attention owing to their high sensitivity and fast response time. Their progress is reviewed here, based on several kinds of important nanowires, for applications such as bio/chemical sensors, gas sensors, photodetectors, and strain sensors. Although Schottky-contacted nanowire sensors deliver excellent performance in these fields, they can be further improved by various methods, including defect engineering, surface modification, the piezotronic effect, and the piezophototronic effect, all of which are discussed here. With regard to practical applications, further efforts are required to address challenges such as the stability, selectivity, ultrafast response, multifunctionality, flexibility, distributed energy supply, and sustainability of Schottky-contacted nanowire sensors. Finally, future perspectives and solutions are discussed.

1. Introduction

The Internet-of-Things (IoT) is vital for intelligent life in the future. The advancement of IoT is closely related to the progress of sensors.[1–3] Sensors are devices that are used to detect or monitor the information of events or changes in the environment. The performance of sensors is highly related to the efficiency and security of IoT.[4,5] The Schottky-contacted sensor, formed by a semiconductor with metal/metal-like materials, is an important member amongst the wide range of sensors.[6]

The interaction between a Schottky sensor and the detected objects usually occur on the surface of semiconductors. Therefore, the structure of semiconductor nanowires, which have high length–diameter ratio, leading to large surface-to-volume ratio, is beneficial for the improvement of the performance of the Schottky sensor. The abundant dangling bonds and defects on the surfaces of semiconductor nanowires lead to a high surface reactivity, which makes the semiconductors very sensitive, especially to any change in the surrounding environment.[7] Additionally, the reduction in dimensionality allows the semiconductor nanowires to exhibit modified physical and chemical properties, which are very different from the semiconductors used in bulk or micrometer scale materials.[8–10] semiconductor nanowires is a promising material for highly sensitive Schottky sensors. They have been widely investigated in the fields of biomolecule detection, gas detection, light detection, strain detection, etc.[11]

Herein, Schottky-contacted sensors based on semiconductor nanowires are summarized in order to provide a systematic understanding. A suitable work function for the metal and electron affinity of semiconductors is the key to form the Schottky junction, which first drives the discussion to the selection of the material. In the next section, the fundamental of high sensitivity in Schottky-contacted nanowire sensors is explained. In Section 4, the functions of a Schottky-contacted nanowire sensor are summarized by categorizing the applications of the sensors. Furthermore, a strategy to improve the performance of a Schottky sensor is discussed. Section 6 consists of the conclusion and future perspectives of this review.

2. Materials Selectivity

Under ideal conditions, without the anomalies and surface states, the Schottky barrier forms if the work function of the metal/metal-like material is different with the electron affinity of the semiconductor. This theory was first systematically proposed by Walter Schottky and Sir Neville Mott in 1939.[12,13] A Schottky barrier is an energy barrier generated by an exchange of carriers at the metal–semiconductor interface. The Schottky barrier height (SBH) can be derived according to the following formula

$$\phi_{Bn0} = \phi_m - \chi \tag{1}$$

$$\phi_{Bp0} = \frac{E_g}{q} - (\phi_m - \chi) \tag{2}$$

where ϕ_{Bn0} and ϕ_{Bp0} are the SBHs for the n-type semiconductor and p-type semiconductor, respectively, ϕ_m is the work function of

J. P. Meng, Prof. Z. Li
CAS Center for Excellence in Nanoscience
Beijing Key Laboratory of Micro–Nano Energy and Sensor
Beijing Institute of Nanoenergy and Nanosystems
Chinese Academy of Sciences
Beijing 100083, China
E-mail: zli@binn.cas.cn
Prof. Z. Li
School of Nanoscience and Technology
University of Chinese Academy of Sciences
Beijing 100049, China
Prof. Z. Li
Center of Nanoenergy Research
School of Physical Science and Technology
Guangxi University
Nanning 530004, China
The ORCID identification number(s) for the author(s) of this article can be found under https://doi.org/10.1002/adma.202000130.

DOI: 10.1002/adma.202000130

the metal, χ is electron affinity of the semiconductor, q is the unit electronic charge, and E_g is the bandgap of the semiconductor. The value of the SBH can be influenced by the choice of contact materials owing to the material specific values of ϕ_m, χ, and E_g.

Metals with high work functions and low resistances, including Cu, Ni, Au, Ag, Pt, Pd, and graphene (metal-like), are usually used to form the Schottky junction for n-type semiconductor.[14] However, the SBH can also be affected by the Fermi level pinning of the semiconductor at the interface of the semiconductor and metal/metal-like material, especially for nanomaterials. The commonly used semiconductive nanowires include Si, GaN, ZnO, SiC, InAs, CdS, carbon nanotubes (CNTs), and GaAs (**Figure 1**).[15–33] The Schottky sensors based on these nanowires are fabricated to detect external signals such as bio-molecules, chemicals, light, and strain.

3. The Origin of Sensitivity in Schottky-Contacted Sensors

Once the Schottky junction is formed, the depletion region is generated on the semiconductor side (**Figure 2**a). The SBH can be modulated via external stimulation. The electrical current passing through the Schottky sensor will change due to the variation of the SBH (Figure 2b). Therefore, information regarding the external stimulation will be obtained.[34]

Upon applying an electrical potential between the semiconductor and the metal, a reverse bias is set up. Under the reverse bias, the current of the Schottky sensor can be determined by the following formula, according to the classic thermionic emission–diffusion theory ($V >> 3kT/q \approx 77$ mV)[35]

$$I_R = SA^* T^2 \exp\left(-\frac{\phi_{B0}}{kT}\right) \exp\left(\frac{\sqrt[4]{q^7 N_D (V + V_{bi} - kT/q)/(8\pi^2 \varepsilon_s^3)}}{kT}\right) \quad (3)$$

$$A^* = \frac{4\pi q m^* k^2}{h^3} \quad (4)$$

where S is the area of the Schottky barrier, A^* is the effective Richardson constant, T is the absolute temperature, ϕ_{B0} is SBH, k is the Boltzmann constant, q is the unit electronic charge, N_D is the doping concentration, V is the applied voltage, V_{bi} is the built-in potential, ε_s is the permittivity of semiconductor, m^* is electron effective mass, and h is the Planck constant.

The depletion layer corresponding to the Schottky barrier area is described as[35]

$$W_D = \sqrt{\frac{2\varepsilon_s}{qN_D}\left(V_{bi} - V - \frac{kT}{q}\right)} \quad (5)$$

The parameters in formula (5) are the same as those in formula (3). In this formula, V is positive for forward bias and negative for reverse bias.

Taking into account formulae (3) and (5), it can be seen that the current has an exponential relationship with the SBH under a fixed reverse bias. The SBH changes under external stimulation at the Schottky junction by light illumination, adsorbed charged biomolecules, adsorbed gas molecules, or strain, resulting in an obvious change in the current in sensor. This is the origin of sensitivity in Schottky-contacted sensors.

Jianping Meng received his Ph.D. from General Research Institute for Nonferrous Metals, China, in 2017, his master's degree from China University of Geosciences (Beijing), China, in 2013, and his bachelor's degree from Liaoning Technical University, China, in 2010. He is currently working as an Assistant Professor at Beijing Institute of Nanoenergy and Nanosystems, Chinese Academy of Science. His research interests include sensors, nanomaterials, and nanogenerators.

Zhou Li is a Professor at the Beijing Institute of Nanoenergy and Nanosystems, and School of Nanoscience and Technology, University of Chinese Academy of Sciences. He received his Ph.D. from Peking University, China, in 2010, and his bachelor's degree from Wuhan University, China, in 2004. His research interests are focused on bioelectronics, nanogenerators, self-powered medical systems, nano-biosensors, and single cell mechanics.

4. Application of Schottky-Contacted Nanowire Sensors

Sensors based on nanowires are widely investigated due to the intrinsic characteristics of a nanowire, including a large surface-to-volume ratio and high surface activity. Additionally, Schottky-contacted sensors, fabricated with semiconductor nanowires, are deemed to be promising devices in IoT due to their high sensitivity. In this section, we overview some examples of Schottky-contacted nanowire sensors in the field of detecting biomolecules, chemicals, gas, light, and strain.

4.1. Bio/Chemical Sensors

Biomedical diagnosis requires novel biosensors that possess high sensitivity, high selectivity, high speed, high stability, and high throughput. The sensitive detection of biomolecules (namely, disease markers) is highly beneficial in diagnosing and treating a disease.[36] Schottky sensors based on Si nanowire, CNT, and ZnO nanowires are fabricated to detect pH, DNA, proteins, and glucose with a high sensitivity.

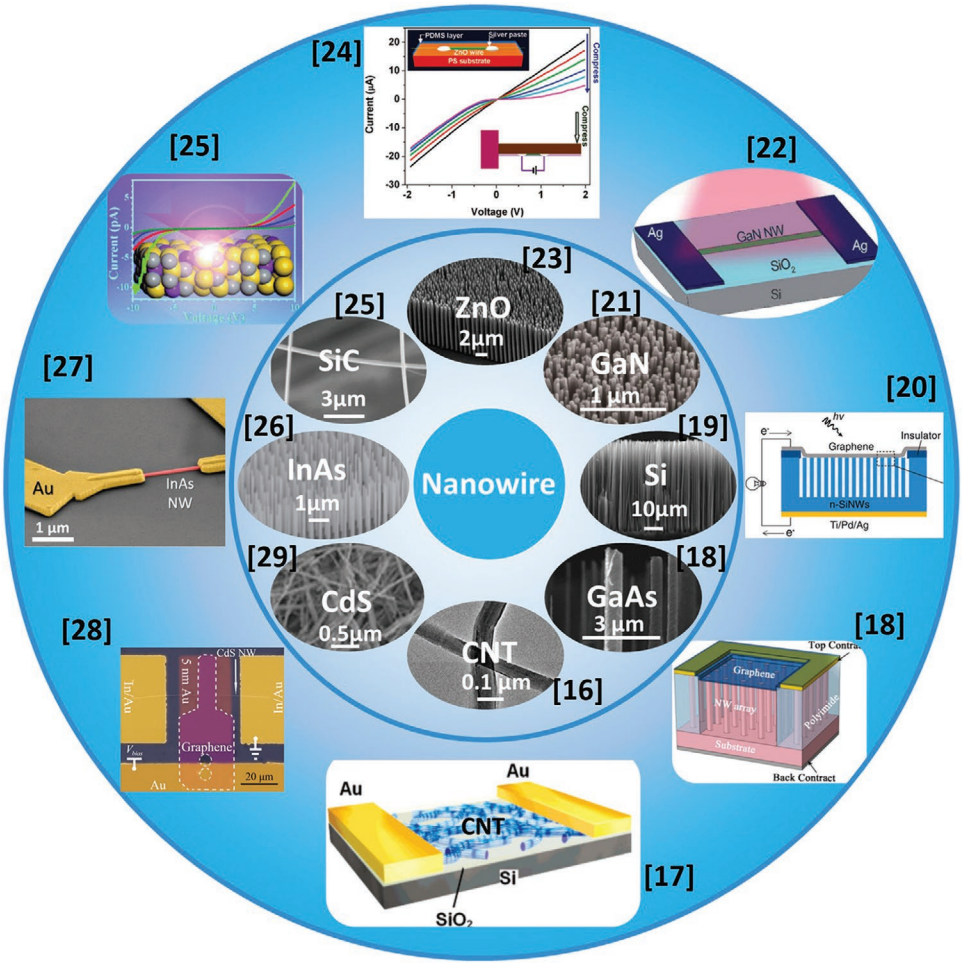

Figure 1. The morphology of semiconductor nanowires and corresponding Schottky-contacted nanowire sensors. Reproduced with permission.[16] Copyright 2015, Royal Society of Chemistry. Reproduced with permission.[17] Copyright 2007, American Chemical Society. Reproduced with permission.[18] Copyright 2016, AIP Publishing. Reproduced with permission.[19] Copyright 2018, Elsevier. Reproduced with permission.[20] Copyright 2011, American Chemical Society. Reproduced with permission.[21] Copyright 2014, Wiley-VCH. Reproduced with permission.[22] Copyright 2014, Royal Society of Chemistry. Reproduced with permission.[23] Copyright 2008, American Chemical Society. Reproduced with permission.[24] Copyright 2008, American Chemical Society. Reproduced with permission.[25] Copyright 2016, Royal Society of Chemistry. Reproduced with permission.[26] Copyright 2013, Elsevier. Reproduced under the terms of the CC-BY Creative Commons Attribution 4.0 International License (http://creativecommons.org/licenses/by/4.0/).[27] Copyright 2019, The Authors, published by MDPI. Reproduced with permission.[28] Copyright 2010, American Chemical Society. Reproduced under the terms of the CC-BY Creative Commons Attribution 4.0 International License (http://creativecommons.org/licenses/by/4.0/).[29] Copyright 2014, The Authors, published by Springer Nature. Source references for each image are indicated in the figure.

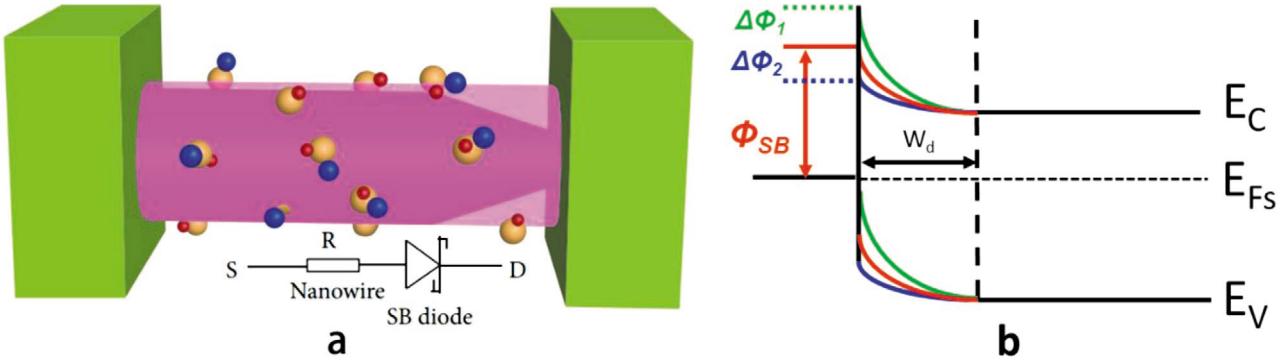

Figure 2. Schematic of the working principle of Schottky sensor. a) The structure of Schottky sensor. b) Change in SBH and depletion region under the external stimulation. a,b) Reproduced with permission.[34] Copyright 2010, Wiley-VCH.

A pH sensor, based on the Schottky junction between a $NiSi_2$ and Si nanowire, was fabricated by Cuniberti and co-workers.[37,38] The charge transport of a Schottky sensor was analyzed theoretically via finite element analysis. In their model, the saturated current increased with an increase in the gate voltage, due to a decrease in the Schottky barrier width. Subsequently, the Schottky sensor, based on parallel arrays of nanowires, was used to detect the pH of a solution. The sensor shows an excellent performance, with a high sensitivity and accuracy, which stems from the Schottky junctions formed by Ni and Si after annealing. The sensor also exhibits good stability and robustness after it is integrated with a portable fluidic system for an experiment carried out over a long period of time. Carrara et al. introduced a Schottky-contacted nanowire sensor, based on a surface functionalized Si nanowire by rabbit antibodies to detect antigens (**Figure 3**a).[39] The activation energy

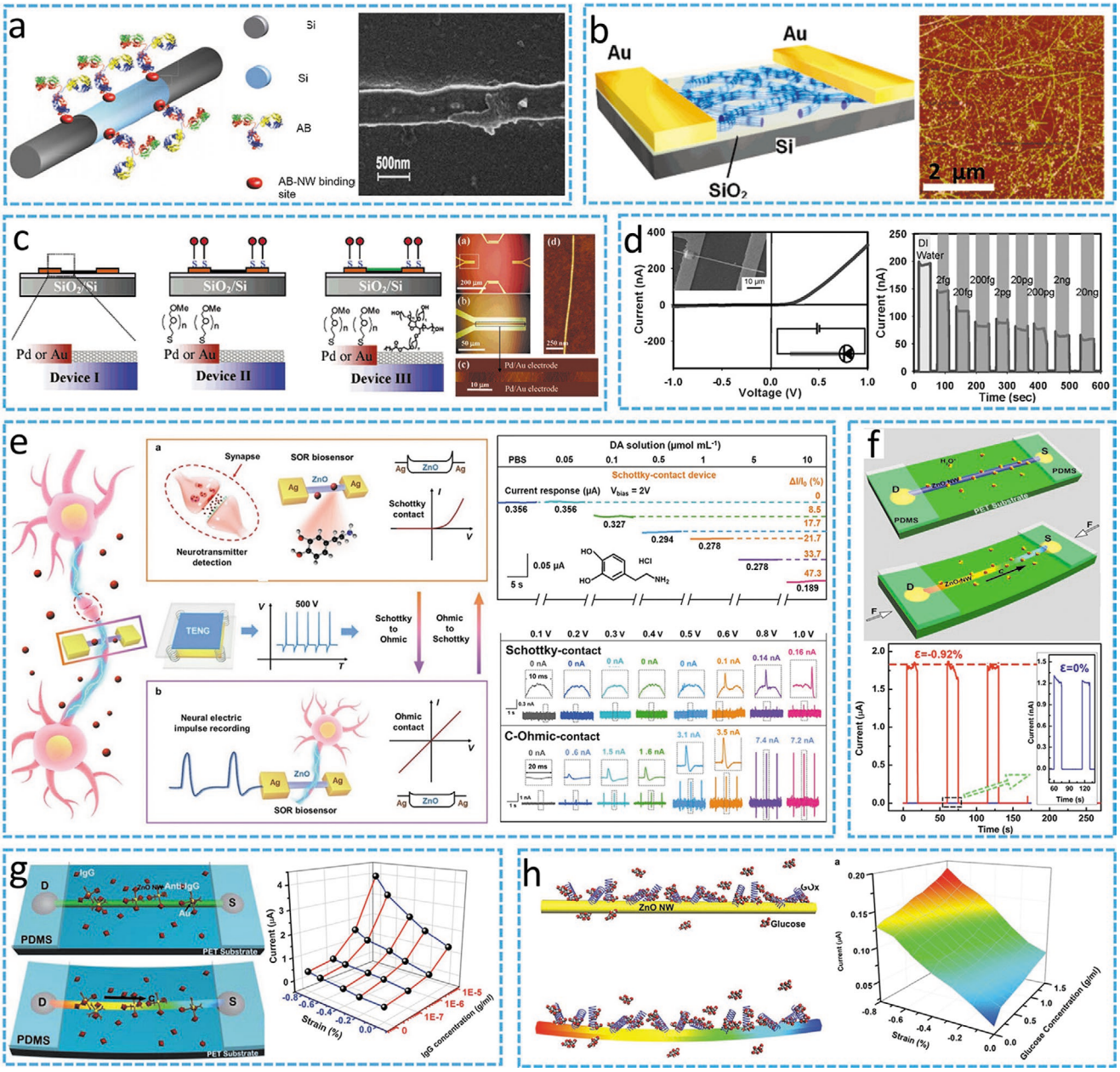

Figure 3. Bio/chemical sensors of Schottky-contacted nanowires. a) Si nanowire with surface functionalized antibodies for antigen detection. Reproduced with permission.[39] Copyright 2012, Elsevier. b) Schottky sensor of CNT for DNA detection. Reproduced with permission.[17] Copyright 2007, American Chemical Society. c) Schottky sensor of CNT for protein detection. Reproduced with permission.[40] Copyright 2004, American Chemical Society. d) Schottky sensor of ZnO nanowire for detecting charged molecules. Reproduced with permission.[41] Copyright 2009, Wiley-VCH. e) Multifunctional ZnO nanowire Schottky sensor for detecting dopamine and neuronal signal. Reproduced with permission.[42] Copyright 2019, Wiley-VCH. f) Schottky sensor of the ZnO nanowire for pH detection. Reproduced with permission.[44] Copyright 2013, American Chemical Society. g) Schottky sensor of the ZnO nanowire for protein detection. Reproduced with permission.[45] Copyright 2013, Royal Society of Chemistry. h) Schottky sensor of the ZnO nanowire for glucose detection. Reproduced with permission.[47] Copyright 2013, Wiley-VCH.

plots reveal that the SBH is 525 meV. The detection limit and sensitivity of the Schottky sensor, in this case, are $(3.4 \pm 1.8) \times 10^{-15}$ M and 37 ± 1 mV fM^{-1}, respectively.

A Schottky sensor, based on Au and single-walled carbon nanotube (SWCNT) networks, is used to detect deoxyribonucleic acid (DNA) (Figure 3b).[17] A low-temperature electrical measurement provides direct evidence that the SBH is affected by DNA immobilization and hybridization. A photoresistance capping investigation indicates that the sensitivity of this Schottky sensor is determined by the change in the Schottky junction based on the metal-SWCNT rather than the channel conductance of SWCNT. Dai and co-workers developed a "micromat" sensor based on a microarray CNT and a Pt/Au Schottky junction (Figure 3c).[40] A systematic investigation is conducted to reveal the mechanism of this structure in the solution-phase biosensing. The sensitivity of the sensor originates from the change in the SBH, owing to biomolecular adsorption. Surface modification is implemented, by passivation with mPEG-SH, to improve the detection of the sensor (pI 10–11) for protein avidin. Combining the Schottky junction between the metal and CNT, and the respective interactions of the proteins, the sensor performance can be further optimized to achieve high sensitivity and selectivity for aqueous-phase biosensing.

Li and co-workers fabricated a ZnO nanowire biosensor based on Schottky contact by photolithography and focus ion beam technology (Figure 3d).[41] This biosensor was highly sensitive with respect to detecting low concentration hemoglobin (2 fg mL^{-1}), unlike the Ohmic contact device, which is insensitive to charged molecules, even if the concentration is up to 800 μg mL^{-1}. The sensitivity of the Schottky sensor originates from the change in the SBH, caused by the adsorption of charged molecules. This Schottky sensor is capable of realizing high sensitivity detection without biological probes, and provides a potential way of proactively detecting charged molecules, as the junction may attract charged molecules.

In 2019, a highly sensitive and multifunctional ZnO nanowire biosensor was developed. It detected both biomolecular signals and neural electrical signals (Figure 3e).[42] The Schottky-contacted nanowire sensor is able to realize a highly sensitive detection of 0.1 μmol mL^{-1} dopamine. After being converted to the Ohmic contact status by the pulse voltage of 350 V from TENG, the same nanowire device also achieves an enhanced sensitivity to neuroelectric signals. This work provides a simple way to achieve the reversible conversion from Schottky to Ohmic contact and is beneficial for the development of multifunctional and high-sensitivity biosensors.

The Wurtzite structured ZnO has the piezoelectric property due to its noncentral symmetric structure. In 2006, the Wang group developed the piezoelectric nanogenerator based on the ZnO nanowire array.[43] Subsequently, the piezotronic effect has been widely used to tune the SBH to enhance the performance of the sensor.[44–47] Pan et al. prepared a back-to-back (metal–semiconductor–metal) Schottky contact ZnO nano/microwire sensor (Figure 3f).[44] This sensor exhibits a high sensitivity toward pH. The sensitivity and signal level of the sensor is increased further by tuning the SBH when the piezopotential is generated by an external strain. The outstanding impact of the piezotronic effect on improving the performance of the Schottky-contacted nanowire sensor is also exhibited by Yu et al.[45] and Cao et al.[46] in their works, wherein they investigate the immunoglobulin G (IgG)-targeted protein (Figure 3g) and the human immunodeficiency virus gene. Furthermore, the target molecules near the micro/nanowire surface can be attracted using electrostatic interaction, due to the nonuniform distribution of the piezopotential along the ZnO micro/nanowire. This allows the sensor to proactively detect low concentrations of target molecules, which is beneficial to the improvement of the sensitivity and lowering of the detection limit.

For the purpose of fabricating a self-powered Schottky-contacted nanowire sensor, Yu et al. investigated the glucose sensing performance of a ZnO nano/microwire based sensor with an integrated triboelectric nanogenerator (Figure 3h).[47] The triboelectric nanogenerator works as the power source of the self-powered glucose monitoring system (GMS). This work provides a guideline to develop a self-powered and distributed GMS.

4.2. Gas Sensors

Air pollution and flammable/explosive gases may threaten people's health or life. A gas sensor can monitor and detect gas species and their concentrations in order to provide warnings.[48] In 1962, Seiyama and a co-worker reported the phenomenon that the conductivity of a semiconductive material can be changed with the injection of a reactive gas.[49] Since then, a tremendous amount of work has been reported on the applications of low-dimensional materials as gas sensors, due to their excellent performance.

Kumar et al. reported a Schottky sensor based on a Pd and ZnO nanowire array to detect hydrogen at low temperatures.[50] Besides serving as a part of the Schottky junction, Pd also works as a catalyst (**Figure 4**a). The sensor performance of diverse gas species such as H_2, CH_4, H_2S, and CO_2, is investigated with a concentration range of 7 ppm to 10 000 ppm (1%) under the temperatures between 50 and 175 °C. The Schottky-contacted nanowire sensor constructed by Pd and ZnO nanorods has a high selectivity to H_2 in the mixing gas. The mechanism is dominated by the activation energy of the target gases and the change of the SBH.

A Schottky/Ohmic sensor formed by Pt and a single ZnO nanowire was used to detect the CO by Wei et al.[51] A comparison of the sensor performance between the Ohmic-contacted nanowire sensor and the Schottky-contacted nanowire sensor was conducted. The Schottky-contacted nanowire sensor achieves a significant improvement in performance with respect to sensing CO, as compared to the performance of the Ohmic contact device (Figure 3b). The response and recovery time can be shortened by a factor of 7. The high sensitivity of the Schottky-contacted nanowire sensor is due to the change of the SBH when the gas is injected into the chamber.

Suehiro et al. fabricated another Schottky sensor based on a single-walled CNT and different metals (Al, Cr, or Pd).[52] The resistance of the Schottky-contacted sensor based on Al and CNT increases when NO_2 is injected into the chamber, whereas the resistance decreases for the sensors based on the other metals (Cr, Pd) and CNT. The adsorbed NO_2 might change the conductivity of CNT and the SBH of Al-CNT (Figure 4c). It has

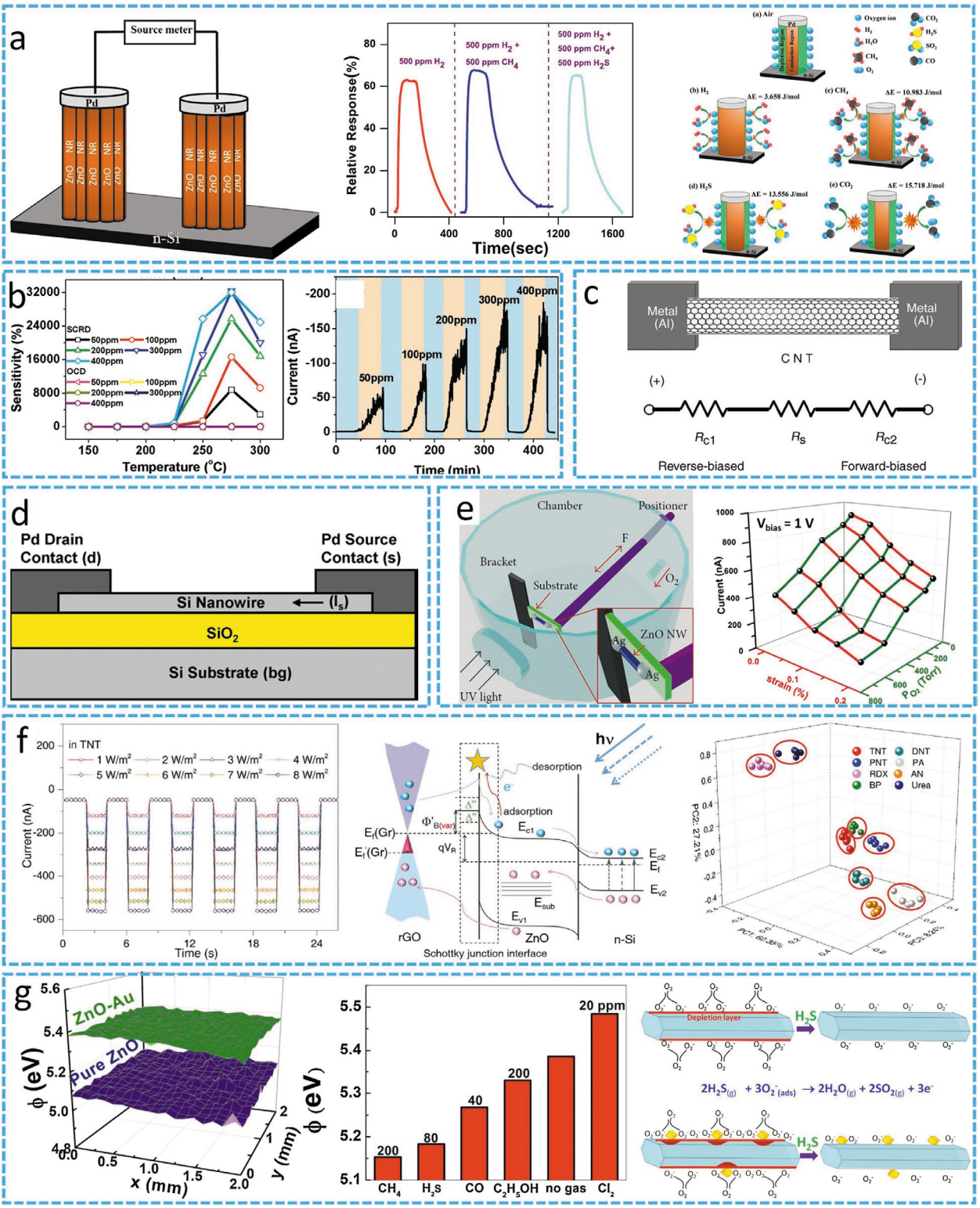

Figure 4. Gas sensor of Schottky-contacted nanowire. a) Hydrogen sensor based on Schottky contact of Pd and ZnO nanorods. Reproduced under the terms of the CC-BY Creative Commons Attribution 4.0 International License (http://creativecommons.org/licenses/by/4.0/).[50] Copyright 2017, The Authors, published by Springer Nature. b) Comparation of sensitivity between Schottky-contacted senor and Ohmic-contacted sensor. Reproduced with permission.[51] Copyright 2009, American Chemical Society. c) Schematic diagram of Al–CNT Schottky contact device and the equivalent circuit. Reproduced with permission.[52] Copyright 2006, Elsevier. d) Schematic of the Schottky sensor of silicon nanowire. Reproduced with permission.[15] Copyright 2018, Elsevier. e) Piezotronic effect enhanced ZnO nanowire oxygen sensor. Reproduced with permission.[54] Copyright 2013, Wiley-VCH. f) rGO/ZnO/SiNWs Schottky gas sensor of explosive vapors. Reproduced with permission.[55] Copyright 2016, Wiley-VCH. g) Au@ZnO Schottky nanowire sensor of H_2S gas. Reproduced with permission.[56] Copyright 2013, Elsevier.

a faster response time than the other metal-CNT sensors due to the Schottky junction. The Schottky-contacted sensor can achieve NO_2 detection of sub-ppm level at room temperature.

Skucha et al. designed a Schottky sensor based on a Pt and Si nanowire array to detect H_2 via the printing process (Figure 4d).[15] The sensor can detect H_2 in the concentration range of 3 ppm to 5% reliably and reversibly. The nanowire array increases the adsorbing area of the gas molecules. The porous nanonetwork gives another method to achieve this target. Zhong et al. fabricated a Schottky sensor based on Pt and a porous GaN nanonetwork for H_2 detection.[53] The *I–V* curve analysis indicates that the ideality factor and SBH of this sensor are 38.5 and 0.497 eV, respectively. This sensor exhibits a good performance in detecting H_2 gas in the range of 320 to 10 000 ppm, at room temperature.

Although the gas sensor of the Schottky contact has a high sensitivity, various methods of improvement (such as piezotronic effect, photoexcitation, surface modification, and element doping) are investigated as effective ways to increase the sensitivity and decrease the work temperature.[54–57]

To achieve oxygen detection at room temperature, oxygen sensors, enhanced via the piezotronic effect, were prepared by Niu et al. (Figure 4e).[54] The sensitivity of the sensor for O_2 was enhanced by tuning the SBH via the piezopotential when a tensile strain was applied.

Light illumination can accelerate the desorption process and also tune the SBH.[58,59] Guo et al. designed a SiNWs (nanowires)/ZnO/rGO Schottky sensor to detect explosive vapors.[55] The sensor exhibits an excellent photoresponse for light having a wavelength of 468 nm under the saturated vapors of 2,4,6-trinitrotoluene (TNT) (Figure 4f). The SBH is changed under the coupled stimulation of light illumination and molecule adsorption. Therefore, a high sensitivity to explosive vapors is achieved (Figure 4f). Each type of explosive vapor can be distinguished by principal component analysis (PCA). This proof-of-concept system can achieve semiquantitative detection of the vapor phase explosives at room temperature.

A noble metal particle, which is a good candidate for a catalyst, can modify the surface of a semiconductor nanowire. It can decrease the working temperature and increase sensitivity. Ramgir et al. achieved the detection of H_2S at room temperature using modified ZnO nanowires with Au particle.[56] Compared to the pure ZnO NWs, the modified ZnO nanowires exhibit a remarkable increase of 16-fold toward the 5 ppm H_2S at room temperature. The pure ZnO nanowires and the modified ZnO nanowires with Au particles have work functions as 5.09 and 5.39 eV, respectively (Figure 4g). The improvement of the performance is due to the change in the SBH in the nano-Schottky junction formed between the Au particles and the ZnO nanowire. Additionally, Au particles as a catalytic material, increase the quantity of oxygen ions on the surface of ZnO NWs, which also can accelerate the reaction process and shorten the response/recovery time. This mechanism of surface modification is also called electronic sensitization or chemical sensitization.[60–62] In a similar fashion, the Ag nanoparticle on the surface of the CdS nanowire can be used for modification, by forming a Schottky junction.[57] The performance of the sensor with respect to detecting ethanol is enhanced after decorating by Ag nanoparticles when the humidity is below 60% RH. The sensor exhibits a high stability after four months.

Besides modification by external elements, intrinsic elements can also be adjusted to enhance the sensor performance. Utilizing surface defect engineering, by adjusting the content of the oxygen element in the SnO_2 nanowire, the performance of the gas sensor based on Pt and SnO_2 nanowire Schottky contact is improved.[63] The surface defect (oxygen vacancy) is generated by tuning the oxygen flow while preparing the SnO_2 nanowire. The sensing performance of the Schottky sensor based on the SnO_{2-X} nanowire is enhanced by 200% with respect to detecting CO in a pure O_2 environment. The response/recovery time is also shortened. This investigation indicates that the sensor performance can be improved extraordinarily by combining the surface oxygen defects and Schottky contact.

The piezotronic effect, photoexcitation, surface modification, heterostructures, and defect engineering are effective methods to improve the performance of a gas sensor.[55–57,63–66] Light illumination can accelerate the desorption process and shorten the recovery time. Functionalization on the nanowire surface with other compounds,[67–69] noble metals,[70–78] and polymers[79–83] is proved to be an effective way to accelerate the recovery process. The formation of a heterojunction by surface modification can passivate the dangling bond and generate a depletion layer on the nanowire surface, which also shortens the recovery time. Additionally, the noble metal particles (Ag,[70] Au,[71–73] Pt,[74–76] Pd,[76–78] etc.), acting as catalytic materials, can accelerate the reaction during the detection process, which can also decrease the working temperature. Element doping can change the gain size, morphology, and carrier concentration of a semiconductor nanowire, which can shorten the response time and improve the performance of the gas sensor as well.[84–86] Furthermore, the generated defect and heterojunction in a semiconductor due to element doping promotes the separation and transportation of carriers.[84,86,87]

4.3. Photodetectors

A photodetector plays a crucial role in wearable electronic devices (such as smart glasses, smart watches, and wearable cameras).[88–90] Using semiconductor nanowires as the photodetector materials has several advantages: 1) large surface-to-volume ratio, 2) deep-level trap states on nanowire surface, and 3) shorter carrier transit time due to the reduced dimensionality of the active area.[8]

Graphene has the metal-like properties of high conductivity coupled with high carrier mobility and high transparency. It is a suitable material to fabricate the Schottky-contacted photodetector with the semiconductor nanowire/nanowire array. Fan et al. designed a Schottky junction solar cell, based on a graphene and Si nanowire array to detect the light and harvest solar radiation (**Figure 5**a).[20] This structure exhibits a strong UV light trapping effect, which can enhance the light absorption. Nie et al. designed a photodetector based on the Schottky junction between monolayer graphene (MG) and a ZnO nanowire array (Figure 5b).[91] The response and recovery time are 0.7 and 3.6 ms, respectively. The sensor exhibits very little sensitivity to visible light. Therefore, the Schottky sensor shows a

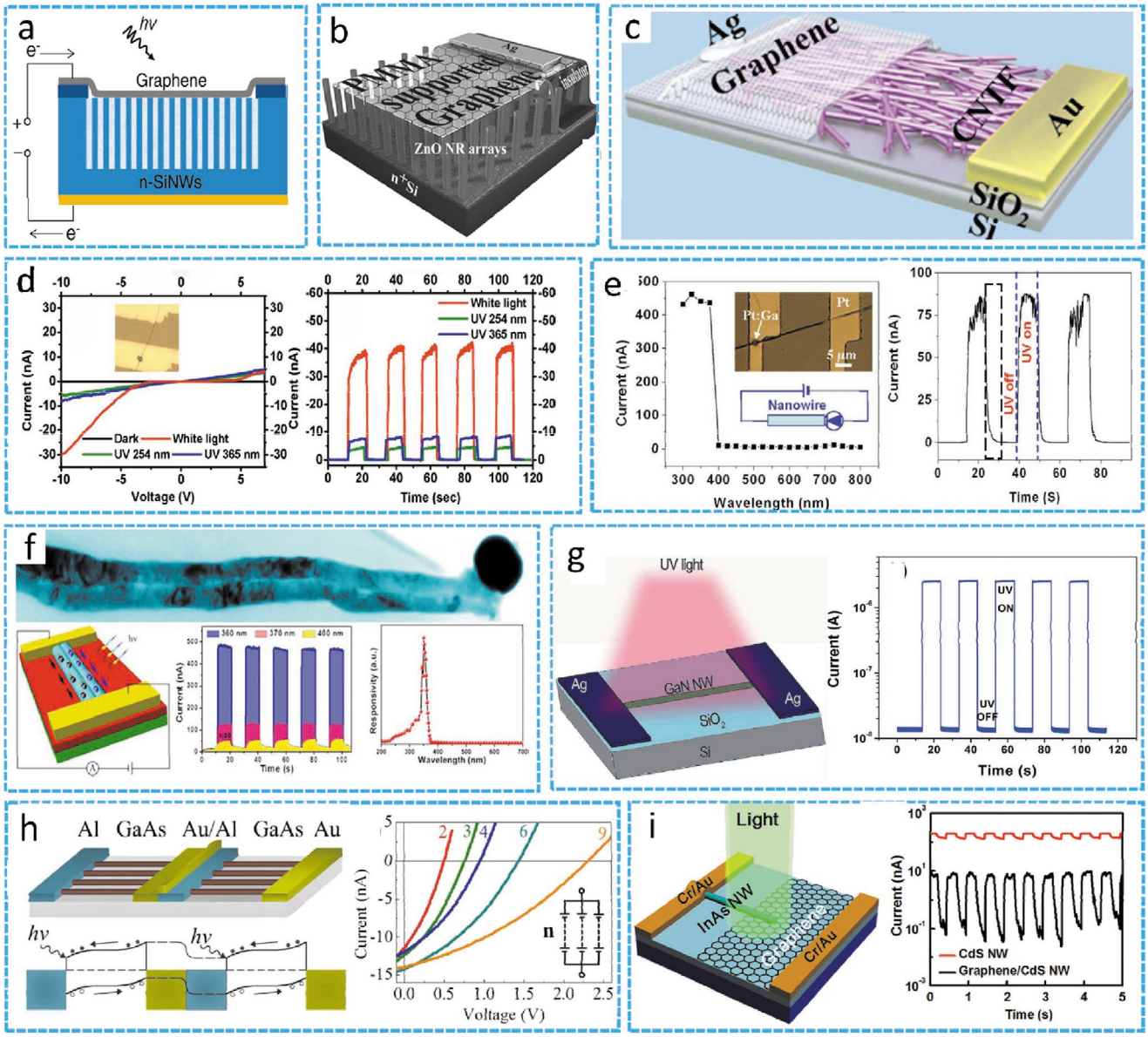

Figure 5. Photodetectors of Schottky-contacted nanowires. a) Schematic of solar cell of Si nanowire. Reproduced with permission.[20] Copyright 2011, American Chemical Society. b) Schematic of UV photodetector consisted of monolayer graphene and ZnO nanowire array. Reproduced with permission.[91] Copyright 2013, Wiley-VCH. c) Schematic of a Schottky photodetector prepared from single-layer graphene and CNT film. Reproduced under the terms of the CC-BY Creative Commons Attribution 4.0 International License (http://creativecommons.org/licenses/by/4.0/).[92] Copyright 2016, The Authors, published by Springer Nature. d) Schottky-contacted CdS nanowire sensor. Reproduced with permission.[93] Copyright 2010, AIP Publishing. e) Photoresponse performance of a ZnO nanowire UV sensor. Reproduced with permission.[94] Copyright 2009, AIP Publishing. f) Structure and performance of a UV photodetector based on a bicrystalline GaN nanowire. Reproduced with permission.[95] Copyright 2017, American Chemical Society. g) Structure and performance of a GaN nanowire-based UV sensor. Reproduced with permission.[22] Copyright 2014, Royal Society of Chemistry. h) Schematic and photoelectric performance of a solar cell based on GaAs nanowire. Reproduced with permission.[96] Copyright 2015, American Chemical Society. i) InAs NW photodetector. Reproduced with permission.[98] Copyright 2014, Wiley-VCH.

high selectivity toward ultraviolet (UV) light. This photodetector can detect a pulsed UV light of 2250 Hz. This demonstrates that the photodetector can realize rapid detection. Besides a vertical array structure, a horizontal array structure was also designed to enhance the performance of the photodetector. A nano-photodetector based on single layer graphene (SLG) and carbon nanotube thin films (CNTF) is sensitive to light in a wide wavelength range (Figure 5c).[92] The response and recovery time are 68 and 78 μs, respectively, under an illumination of 980 nm (166 mW cm^{-2}). Meanwhile, the responsivity is 209 mA W^{-1} at the bias of 3 V. This nano-photodetector has a potential application in nano-optoelectronic devices and systems.

Besides the nanowire array, Schottky photodetectors based on individual nanowires have also been investigated widely. A Schottky photodetector having Au/Ag and a single-wall CNT was prepared by Chen et al.[32] In this Ag–CNT–Au Schottky

detector, holes and electrons are separated by built-in potential at the Ag–CNT Schottky contact. Then, the separated electrons and holes only need to pass through a small barrier between Au and the nanotube before being collected. This asymmetric structure demonstrates a high performance for infrared (IR) waves. Wei et al. fabricated another CdS Schottky-contacted nanowire sensor to detect visible light (Figure 5d).[93] The Schottky-contacted nanowire sensor shows a high sensitivity of 10^5% to visible light, whereas the Ohmic-contacted nanowire sensor shows a weak sensitivity to visible light. This performance enhancement stems from the Schottky junction. Zhou et al. compared the performance of the Ohmic-contacted and Schottky-contacted UV sensors based on individual ZnO nanowires.[94] The Schottky-contacted UV sensor exhibits four orders of magnitude improvement of sensitivity. The reset time is only ≈0.8 s (Figure 5e). By surface modification, the reset time can be reduced to ≈20 ms. Their work shows a significant approach for constructing a UV detector with the features of fast recovery and high response. Zhang et al. synthesized the bicrystalline GaN nanowires by the catalytic method to design a high performance photodetector.[95] This photodetector, based on the Schottky junction of Au and single bicrystalline GaN nanowire, exhibits a high photoresponsivity of 1.74×10^7 A W^{-1} and a photoresponse time of 144 ms (Figure 5f). The two separated crystals in the GaN nanowire provide a channel for carrier separation and transportation, which leads to an enhanced performance of the photodetector. This work demonstrates that a grain boundary in the semiconductor is beneficial to the carrier separation and transportation. To avoid performance degradation due to surface polarity, a single crystal GaN nanowire with a nonpolar a-axial is used to fabricate a Schottky-contacted UV detector.[22] Its sensitivity is 10^4 A W^{-1} and response time is less than 26 ms (Figure 5g). This excellent performance renders the sensor as an optical logic device and future memory storage.

GaAs and InAs nanowire, which are narrow band gap semiconductors, have a high absorption coefficient, high carrier concentration, and high carrier mobility. They are usually used for infrared detection and photoelectric conversion. GaAs nanowire is configured into a novel Schottky photovoltaic device to harvest solar radiation by using the Al and Au electrode.[96] A single wire device can achieve the energy conversion efficiency of 16% under light illumination at an air mass of 1.5. Integrating individual devices into series, the overall efficiency reaches up to 1.6%. This device can be fabricated into a transparent and flexible photovoltaic on a transparent substrate for next-generation smart solar energy harvesting devices. Combining the high carrier mobility and high transparency, the photodetectors based on the Schottky junction between graphene and GaAs/InAs nanowire are investigated (Figure 5i).[97,98] The photoresponsivity of the GaAs nanowire based sensor is 231 mA W^{-1} under 532 nm laser illumination, and it has a fast response/recovery time of 85/118 µs. The good performance of the photodetector stems from the strong built-in potential and the excellent carrier transparent property. These results provide ways to develop graphene-based electronics, optoelectronics, and photonics. The performance summary of photodetectors is shown in **Table 1**.

It is extremely essential to improve the performance of the photodetector, which is significant to environmental sensing and optical communication. The piezophototronic effect,[99–102] pyroelectric effect,[103–110] and surface modification[111–114] are effective ways to improve the photodetector performance.

Lu et al. investigated the enhanced performance of the UV sensor based on the Au–ZnO Schottky junction detector by utilizing the piezotronic effect (**Figure 6**a).[99] The sensitivity can be increased by 500% by applying a tensile strain of 0.580%. The produced piezopotential enhances the built-in field, which strengthens the separation of the electron-hole pairs generated by photoexcitation. Using the same method, the sensitivity of this Ag/ZnO nano/microwire Schottky photodetector is enhanced, by piezophototronic effect, more than fivefold with respect to sensing UV light of low power density of pW levels.[100] These important proof of concepts provide a significant progress to boost the performance of the photodetector dynamically. The phenomenon of this performance enhancement by the piezophototronic effect is also observed in the Schottky photodetector prepared from the GaN nanowire array[101] and ZnO nanowire array (Figure 6b).[102] The piezophototronic effect can improve the performance of the Schottky photodetector based on the single nanowire and nanowire array as well.

The piezophototronic effect can enhance the photoresponsivity and sensitivity of the Schottky-contacted nanowire sensor. In addition, introducing the pyroelectric effect into the photodetector can tune the transportation of the carriers in the photoelectric process faster, which can shorten the response and recovery time of the photodetector noticeably.[103–110] Wang et al. systematically investigated the influence of the pyrophototronic effect on the performance of the photodetector based on Ag and ZnO nanowire Schottky junction.[103] Coupling the pyroelectric effect, the photodetector exhibits a transient photoresponsivity of 1.25 mA W^{-1} under 325 nm light illumination. It is enhanced

Table 1. Performance of Schottky-contacted nanowire photodetectors.

Materials	Bias [V]	Wavelength [nm]	Photoresponsivity [A W^{-1}]	Sensitivity	On/off ratio	Response/recovery time	Ref.
MG and ZnO nanowire array	−1	365	113	–	–	0.7/3.6 ms	[91]
SLG and CNTF	−3	980	0.209	–	100	68 µs/78 µs	[92]
Pt–CdS	−8	254/325		≈10^5%		/<320 ms	[93]
Pt–ZnO	1	365	–	–	–	/<20 ms	[94]
Au and bicrystalline GaN nanowire	5	320–400	1.74×10^7	–	203	144/256 ms	[95]
Ag and GaN nanowire	1	325	<10^4	–	–	<26 ms	[22]
Graphene and InAs nanowire	–	532	0.5	–	5×10^2	–	[98]

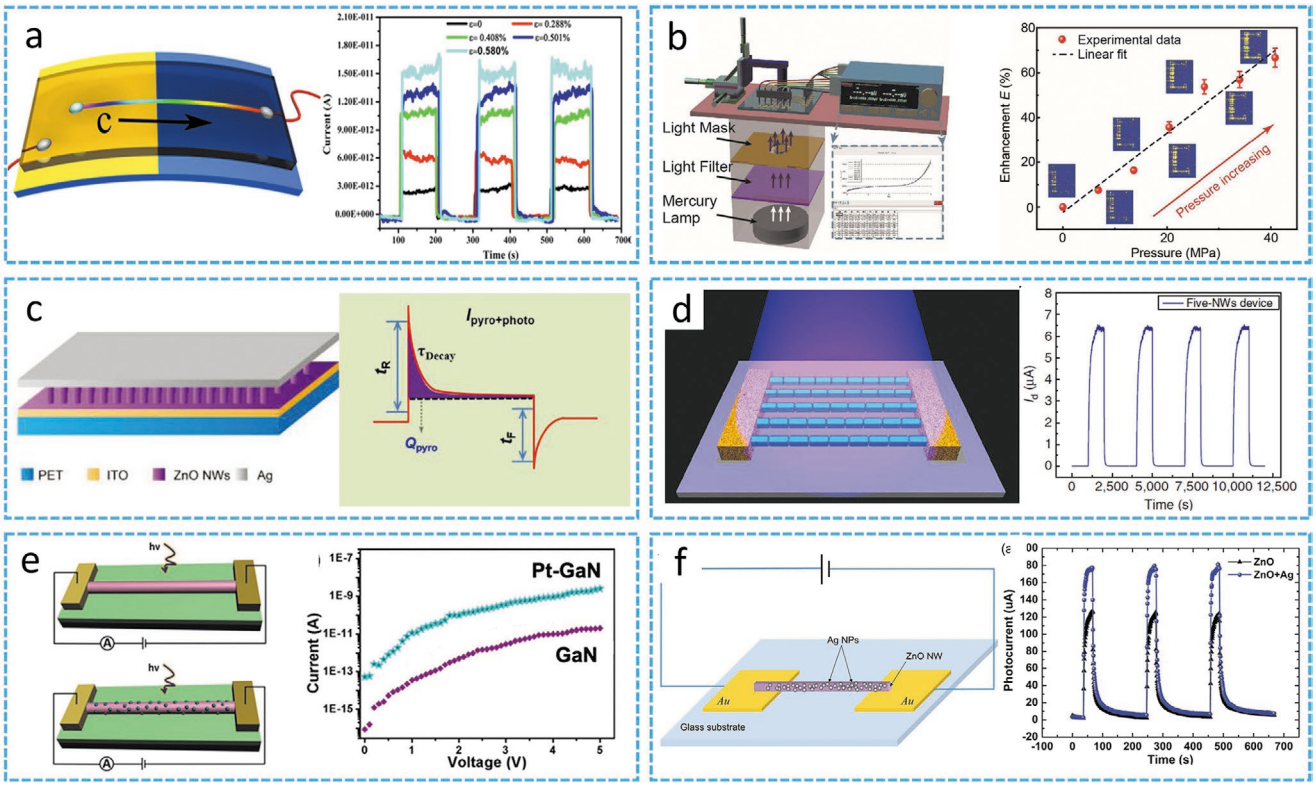

Figure 6. Enhanced performance of Schottky-contacted photodetectors. a) Piezotronic enhanced performance of a Au/ZnO nanowire photodetector. Reproduced with permission.[99] Copyright 2014, American Chemical Society. b) Piezophototronic enhanced UV sensing array. Reproduced with permission.[102] Copyright 2015, Wiley-VCH. c) Pyrophototronic-effect-enhanced self-powered photodetector based on Ag and ZnO Schottky contact. Reproduced with permission.[103] Copyright 2018, Wiley-VCH. d) Schematic and performance of a UV photodetector prepared from ZnO granular nanowires. Reproduced with permission.[111] Copyright 2014, Springer Nature. e). Enhanced performance of a Schottky photodetector comprising GaN nanowire decorated with Pt particles. Reproduced with permission.[112] Copyright 2014, Royal Society of Chemistry. f) Enhanced performance of Schottky photodetector prepared from a ZnO nanowire decorated with Ag particles. Reproduced with permission.[113] Copyright 2014, Royal Society of Chemistry.

by 1465% as compared to the steady-state signal. This work studies the pyrophototronic coupling effect in the different stages of light detection, which gives new clarification regarding the fundamentals of the pyrophototronic effect and promotes the performance of new photodetectors.

The surface trap state of a semiconductor nanowire can prolong the lifetime of the photocarrier. The performance of the photodetector can be further improved by modifying the band edge. Liu et al. reported a high-performance photodetector, based on a polycrystalline nanowire, via band edge engineering (Figure 6d).[111] The prepared device shows an ultra-high detectivity of 3.3×10^{17} Jones. A systematic study indicates that the performance of the device is attributed to the modification of the band edge. The series Schottky junction along the axial direction of the nanowire results in a high suppression of dark current. The photocurrent rises rapidly from 20 pA to 6.5 μA at 1 V bias once the light is on, and falls equally rapidly. The discovered principle offers a guideline to develop high-performance photodetectors by using other nanomaterials.

The photodetector performance can be improved by decorating the noble metal on the surface of the semiconductor to form a heterojunction.[112–114] Using Pt nanoparticle (NP) modification, the UV photoresponse, based on the Schottky junction of a single GaN nanowire, is greatly improved.[112] The photoresponsivity is enhanced from 773 to 6.39×10^4 A W^{-1}. The external quantum efficiency (EQE) is increased from 2.71×10^5% to 2.24×10^7%. After Pt NP modification, the response time and recovery time of the photodetectors have been largely shortened from 17.5 to 1.1 s and from 6.2 to 0.65 s, respectively. Besides forming a Schottky contact, another main factor is that the Pt nanoparticle on the surface can improve the light absorption due to the effect of localized surface plasmon resonance (LSPR) under UV illumination. The enhancement of the performance by the LSPR effect can also be realized in the Au–ZnO nanowire–Au Schottky photodetector using an Ag nanoparticle decorated ZnO nanowire (Figure 6f).[113] Besides the LSPR effect, the Schottky contact between the Ag nanoparticle and the ZnO nanowire can suppress the recombination of the photogenerated electron–hole pairs sufficiently. Coupling the LSPR effect and piezophototronic effect, the performance can be enhanced further.[114] The performance summary of the above work is shown in **Table 2**.

4.4. Strain Sensors

Structural health monitoring provides a significant contribution to reducing costs by providing early warning signs of major failures. Preventative maintenance programs are necessary for reducing property damage and casualties. Dynamic strain

Table 2. Enhanced performance of Schottky-contacted nanowire photodetectors.

Materials	Bias [V]	Wavelength [nm]	Photoresponsivity [A W^{-1}]	Sensitivity [%]	Response/recovery time	Ref.
Au and ZnO nanowire	0	325	113	≈10^3	≈0.1 s	[99]
Au and ZnO nanowire array	1	365	≈10^4	–	62 ms	[102]
Ag and ZnO nanowire array	0	325	1.25×10^{-3}	≈10^5	4.5 ms/3.5 ms	[103]
Ag and ZnO granular nanowire	1	365	7.5×10^6	–	0.56 s/0.32 s	[111]
Au and GaN nanowire	5	380	6.39×10^4	–	1.1 s/0.65 s	[112]
Au and ZnO nanowire	5	365	4.91×10^6	–	6.3 s/26.3 s,	[113]

sensors play a key role in monitoring the structural health by providing real-time feedback on the integrity of a mechanical structure. The Schottky-contacted nanowire sensor, based on piezoelectric material, is a promising device for the same. This is because the current of the device changes vastly upon tuning the SBH due to the piezopotential, once a strain is generated in the piezoelectric material. For a nanowire, a huge deformation can be achieved before a fracture caused by an external force. In this part, the application of a strain sensor based on a semiconductor nanowire with the piezotronic effect is reviewed.[115–121]

In 2008, Zhou et al. investigated the strain sensor based on individual ZnO nanowires (**Figure 7**a).[115] The generated piezopotential in the ZnO nanowire can proportionately change the SBH, which has a linear relationship with the strain. The *I*–*V* curve shows that the sensor is highly sensitive to strain. The gauge factor of this strain sensor goes up to 1250, which is 25% higher than the corresponding performance of the CNT. This strain sensor has a great potential in the areas of structure/earthquake monitoring, cell biology, and biomedical sciences. Zhang et al. utilized ZnO nanowire arrays to fabricate the high sensitivity strain sensor (Figure 7b).[116] The strain-induced piezopotential can tune the SBH of Au–ZnO, which results in a change in the device conductivity. Here, the gauge factor goes up to 1813. This strain sensor exhibits a robust performance at different frequencies (Figure 7b).

Owing to the high value of polarization in $ZnSnO_3$, a high-performance piezotronic strain sensor based on $ZnSnO_3$ nanowires/microwires was designed by Wu et al. (Figure 7c).[117] Under the small variation of the compressive and tensile strain, the obvious change of SBH leads to a significant change in the device conductivity. This strain sensor achieves a gauge factor of up to 3740. The on/off ratio of the device is ≈587. By doping indium into ZnO, Zhang et al. synthesized the nanobelt with a monopolar surface (Figure 7d).[118] The strain sensor shows a static potential by coupling the Poisson effect and piezotronic effect. This strain sensor exhibits a great gauge factor of 4036 under compressive strain. Under periodical strain measurement, the sensor shows a clear pulse current indicating the response (Figure 7d). The key parameters of these strain sensors are summarized in **Table 3**.

5. Performance Improvement of Schottky-Contacted Nanowire Sensors

The intrinsic junction formed by the metal and the semiconductor nanowire renders the Schottky-contacted nanowire sensor with a high performance, with respect to sensitivity, response time, etc., compared to the performance of the Ohmic-contacted nanowire sensor. Many methods are still investigated to further improve the performance of the Schottky-contacted nanowire sensor. Here, we introduce some general methods, including defect engineering, surface modification, the piezotronic effect, and the piezophototronic effect (**Figure 8**).

5.1. Defect Engineering

The properties of a semiconductor (including carrier concentration and carrier transportation) can be changed via defect engineering. Increasing the surface oxygen vacancy of SnO_2 nanowire can improve the photoresponse and gas sensing performance of the Schottky-contacted nanowire sensor consisting of Pt and SnO_{2-X}.[63] The performance of the photodetector can be vastly improved by introducing a grain boundary into the GaN/ZnO nanowire by synthesizing the polycrystalline structure.[95,111] One of reasons for this lies in the fact that a grain boundary in the nanowire provides independent carrier transfer channels.[95] Another reason is that the band edge is modulated.[111] The performance of the sensor can be improved by defect engineering, not only on the surface, but also on the internal aspects of the material. Additionally, element doping is also an effective method to change the morphology and modulus of the material without losing its electrical performance, by controlling the element concentration.[118,122]

5.2. Surface Modification

The high surface-to-volume ratio of a semiconductor endows it with an abundant surface state, such as dangling bonds. During the detecting process, the interaction of the external stimulation (including molecule, light illumination, and strain) and the sensor mainly occurs on the nanowire surface around the Schottky junction. The surface state can then be modified by forming heterojunctions via introducing other materials onto the surface of the nanowire. Therefore, the performance of the biosensor,[40] gas sensor,[56,57] and photodetector[112–114] can be enhanced by this method. Additionally, forming periodic microstructures on the surfaces of these materials by micro/nanofabrication will improve the gas detection and light absorption via the resonance effect.[123–125]

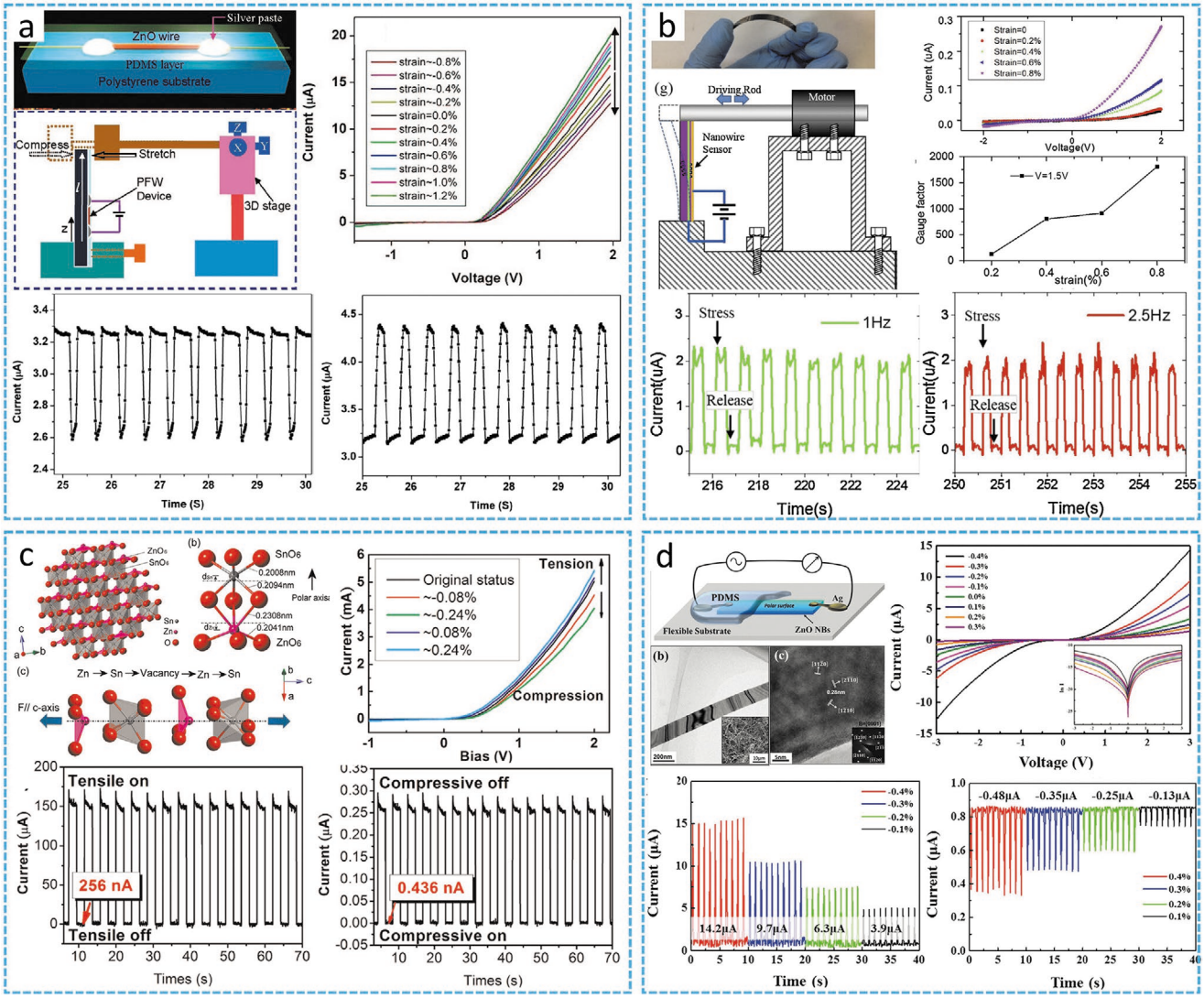

Figure 7. Strain sensors of Schottky-contacted nanowires. a) Strain sensor of a ZnO nanowire. Reproduced with permission.[115] Copyright 2008, American Chemical Society. b) Strain sensor of a ZnO nanowire array. Reproduced with permission.[116] Copyright 2014, Elsevier. c) Strain sensor of a $ZnSnO_3$ nanowire. Reproduced with permission.[117] Copyright 2012, American Chemical Society. d) Strain sensor of an In–ZnO nanobelt. Reproduced with permission.[118] Copyright 2015, Royal Society of Chemistry.

5.3. Piezotronic Effect and Piezophototronic Effect

For a semiconductor nanowire with a noncentral symmetric structure, such as ZnO, GaN, CdS, ZnSe, and quartz, the piezopotential can be produced when a deformation is generated by applying a force along its the direction of its asymmetry. As reported, the piezopotential can tune the SBH, while also modifying the carrier distribution and transportation in Schottky sensors. The schematic of the energy band diagram is used to illustrate the effect of piezoelectric polarization (**Figure 9**).[126–129]

The piezotronic[130] and piezophototronic[131] effects are widely used to improve the performance of the Schottky-contacted nanowire sensor in biomolecule detection,[44–47] gas detection,[54] light detection,[99–102] and strain monitoring.[115–121]

Table 3. Comparison of the key parameters for strain sensor in previous report.

Materials	Response time	Gauge factor	Ref.
Ag/single ZnO nanowire	10 ms	1250	[115]
Au/ZnO nanowire arrays	<100 ms	1813	[116]
Ag/single $ZnSnO_3$ nanowire	–	3740	[117]
Ag/single ZnO nanobelt	≈120 ms	4036	[118]
Au–ZnO nanowire	–	81	[119]
Ag/single ZnO nanowire	≈500 ms	–	[120]

5.4. Others

Besides the methods mentioned above, providing light illumination in the area of Schottky junction can tune the SBH to

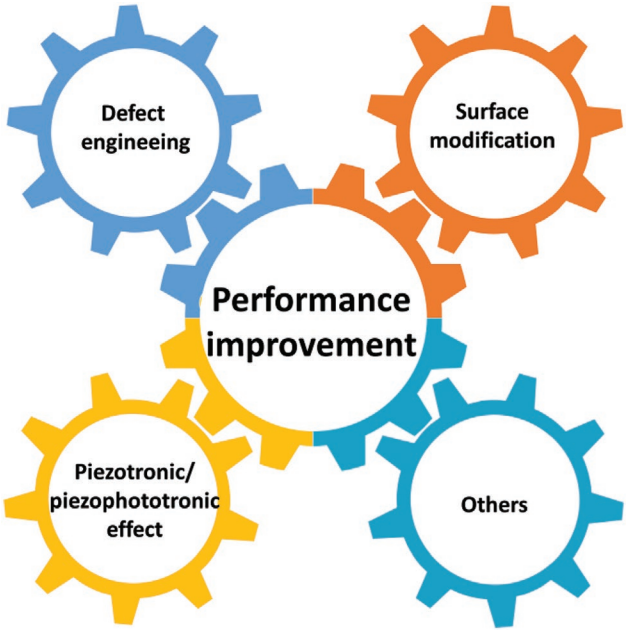

Figure 8. Performance improvement of Schottky-contacted nanowire sensors.

improve the performance of the sensor.[55,132] Additionally, it can also accelerate the desorption process of the gas sensor[55] and improve its performance. Applying a high intensity electric field, generated by an external voltage, on Schottky junction can lower the SBH considerably due to the image lowering effect (Schottky effect).[133,134] In addition, the phenomenon that a high intensity electric field can drive the oxygen vacancy diffusion in ZnO nanobelts is reported.[135] Recently, it has been reported that the diffusion of oxygen vacancies in a ZnO nanowire can be driven by the high voltage of a triboelectric nanogenerator, which can enhance the performance of the sensor by tuning the SBH.[42]

These methods can be effective individually, or can work together by the coupling effect. The piezotronic effect and surface modification are coupled to improve the performance of the sensor.[136] CdS is grown on the surface of a ZnO nanowire to form a core–shell structure. The Schottky sensor based on the CdS@ZnO nanowire exhibits an excellent photoresponse to the visible (548 nm) and UV light (372 nm). Applying a compressive strain, the performance of this photodetector is further improved (**Figure 10**). By coupling surface modification and the piezophototronic effect, the photodetection range of this sensor is expanded to include visible light.

6. Conclusion and Future Perspectives

The Schottky-contacted nanowire sensor receives extensive attention due to the intrinsic high sensitivity of the Schottky sensor and the high surface-to-volume ratio of the nanowire. In this work, we review the recent progress of Schottky-contacted nanowire sensors applied in the fields of bio/chemical molecule detection, gas detection, photodetection, and strain detection. The commonly used metals and semiconductor nanowires are listed. Subsequently, the origin of the sensitivity in Schottky-contacted nanowire sensors is discussed. Finally, the methods of improving the performance of Schottky-contacted nanowire sensors are reviewed.

Although the Schottky-contacted nanowire sensor performs well, there is still a long way to go before it can be promoted for further practical applications. More investigations are needed to inspire efforts to address challenges such as stability, selectivity, speed, and multifunctionality.

First, the high surface-to-volume ratio of the semiconductor nanowire leads to a large contact area. However, it inevitably suffers from the influence of stimulation from the ambient environment. Improving the stability of Schottky-contact nanowire sensors needs to be researched in order to promote this issue. Device encapsulation will be an effective method to address this problem. The second bottleneck to overcome is selectivity, especially for bio/chemical and gas sensors. Surface functionalization can improve the selectivity of the sensor by decorating a functional particle or a specific molecule.[40,137] For example, Pd has exclusive selectivity toward H_2 gas due to the lattice expansion[138]; the unique semiconductor-metal conversion mechanism makes CuO exhibit a high selectivity toward H_2S.[139] Additionally,

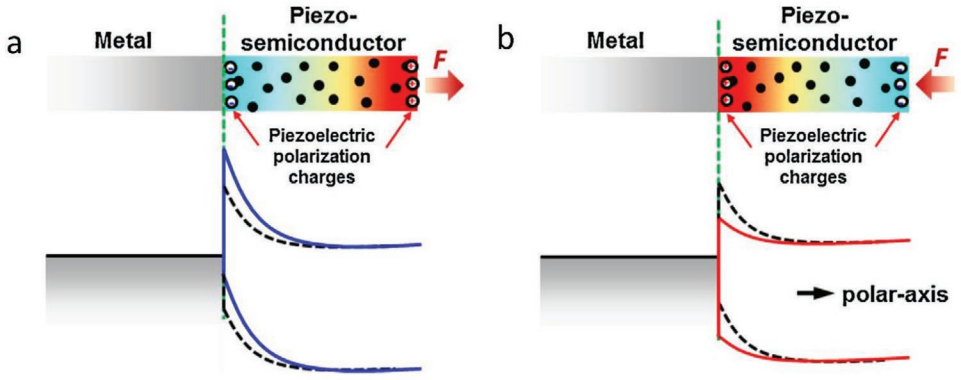

Figure 9. a,b) Schematic of energy band diagram and the change of SBH under the tensile strain (a) and compressive strain (b). a,b) Reproduced with permission.[126] Copyright 2013, Elsevier.

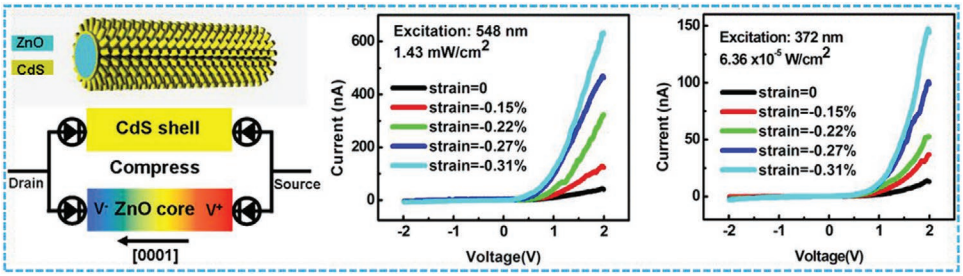

Figure 10. Structure and photoresponse of Schottky-contacted CdS@ZnO nanowire photodetector. Reproduced with permission.[136] Copyright 2012, American Chemical Society.

graphene, CNTs, and conducting polymers can be used to modify the surface of a nanowire for improving the sensor selectivity.[137] The third challenge is shortening the response and recovery time of the Schottky-contacted nanowire sensor to meet the need of real-time detection and future monitoring. The piezotronic effect, piezophototronic effect, and surface modifications may make special contributions to this issue. Another challenge is developing multifunctional sensors to satisfy the varied requirements in complex circumstances. One solution is modifying the nanowire (such as element doping), which can endow the semiconductor nanowire with additional properties.[140] Another solution is the integration of sensors with a single function. The flexibility of the Schottky-contacted nanowire sensor is a key feature for any wearable and implantable electronic device. Several approaches, such as optimization of the structural design, developing intrinsically flexible materials with low Young's moduli, and the integration of individual sensors on a mechanically flexible substrate, can be considered to achieve flexibility.[141,142]

The energy consumption of the Schottky-contacted nanowire sensor is also important for the distribution sensor network in IoT. A self-powered sensor or a lower energy consumption sensor will be the research hotspot in the future. A nanogenerator is a perspective technology that can convert small/micro mechanical work to electric energy in the environment.[143,144] Diverse progresses and applications have been introduced recently, such as wearable/implantable sensors,[145,146] human motion sensors,[147] and marine sensors.[148] A nanogenerator has great potential for constructing the self-powered sensor system, which will exert a profound effect on the future distribution sensor network of IoT.

Acknowledgements

The authors are thankful to National Key R&D Project from Minister of Science and Technology, China (2016YFA0202703), National Natural Science Foundation of China (Nos. 61875015, 81971770, and 21801019), the Beijing Natural Science Foundation (7204333), and the National Youth Talent Support Program for their support.

Conflict of Interest

The authors declare no conflict of interest.

Keywords

biosensors, gas sensors, nanowire sensors, photodetectors, Schottky contact

Received: January 7, 2020
Revised: March 16, 2020
Published online:

[1] D. Miorandi, S. Sicari, F. De Pellegrini, I. Chlamtac, *Ad Hoc Netw.* **2012**, *10*, 1497.
[2] J. Gubbi, R. Buyya, S. Marusic, M. Palaniswami, *Future Gener. Comput. Syst.* **2013**, *29*, 1645.
[3] J. Zhu, X. Liu, Q. Shi, T. He, Z. Sun, X. Guo, W. Liu, O. B. Sulaiman, B. Dong, C. Lee, *Micromachines* **2020**, *11*, 7.
[4] L. Atzori, A. Iera, G. Morabito, *Comput. Networks* **2010**, *54*, 2787.
[5] M. Walshe, G. Epiphaniou, H. Al-Khateeb, M. Hammoudeh, V. Katos, A. Dehghantanha, *Ad Hoc Netw.* **2019**, *95*, 101988.
[6] R. Yu, S. Niu, C. Pan, Z. L. Wang, *Nano Energy* **2015**, *14*, 312.
[7] A. Gurlo, *Nanoscale* **2011**, *3*, 154.
[8] C. Soci, A. Zhang, B. Xiang, S. A. Dayeh, D. P. R. Aplin, J. Park, X. Y. Bao, Y. H. Lo, D. Wang, *Nano Lett.* **2007**, *7*, 1003.
[9] A. Kolmakov, M. Moskovits, *Annu. Rev. Mater. Res.* **2004**, *34*, 151.
[10] L. N. Quan, J. Kang, C. Z. Ning, P. Yang, *Chem. Rev.* **2019**, *119*, 9153.
[11] X. Zhao, R. Zhou, Q. Hua, L. Dong, R. Yu, C. Pan, *J. Nanomater.* **2015**, *2015*, 1.
[12] N. F. Mott, *Proc. R. Soc. London* **1939**, *171*, 27.
[13] W. Schottky, *Z. Phys.* **1939**, *113*, 367.
[14] H. B. Michaelson, *J. Appl. Phys.* **1977**, *48*, 4729.
[15] K. Skucha, Z. Fan, K. Jeon, A. Javey, B. Boser, *Sens. Actuators, B* **2010**, *145*, 232.
[16] H. W. Chang, Y. R. Lu, J. L. Chen, C. L. Chen, J. F. Lee, J. M. Chen, Y. C. Tsai, C. M. Chang, P. H. Yeh, W. C. Chou, Y. H. Liou, C. L. Dong, *Nanoscale* **2015**, *7*, 1725.
[17] E. L. Gui, L.-J. Li, K. Zhang, Y. Xu, X. Dong, X. Ho, P. S. Lee, J. Kasim, Z. X. Shen, J. A. Rogers, Mhaisalkar, *J. Am. Chem. Soc.* **2007**, *129*, 14427.
[18] Y. Wu, X. Yan, X. Zhang, X. Ren, *Appl. Phys. Lett.* **2016**, *109*, 183101.
[19] J. Baek, B. Jang, M. H. Kim, W. Kim, J. Kim, H. J. Rim, S. Shin, T. Lee, S. Cho, W. Lee, *Sens. Actuators, B* **2018**, *256*, 465.
[20] G. Fan, H. Zhu, K. Wang, J. Wei, X. Li, Q. Shu, N. Guo, D. Wu, *ACS Appl. Mater. Interfaces* **2011**, *3*, 721.
[21] C. H. Wang, W. S. Liao, Z. H. Lin, N. J. Ku, Y. C. Li, Y. C. Chen, Z. L. Wang, C. P. Liu, *Adv. Energy Mater.* **2014**, *4*, 1400392.
[22] X. Wang, Y. Zhang, X. Chen, M. He, C. Liu, Y. Yin, X. Zou, S. Li, *Nanoscale* **2014**, *6*, 12009.

[23] S. Xu, Y. Wei, M. Kirkham, J. Liu, W. Mai, D. Davidovic, R. L. Snyder, Z. L. Wang, *J. Am. Chem. Soc.* **2008**, *130*, 14958.
[24] J. Zhou, P. Fei, Y. Gu, W. Mai, Y. Gao, R. Yang, G. Bao, Z. L. Wang, *Nano Lett.* **2008**, *8*, 3973.
[25] X. Li, S. Chen, P. Ying, F. Gao, Q. Liu, M. Shang, W. Yang, *J. Mater. Chem. C* **2016**, *4*, 6466.
[26] M. H. Madsen, P. Krogstrup, E. Johnson, S. Venkatesan, E. Mühlbauer, C. Scheu, C. B. Sørensen, J. Nygård, *J. Cryst. Growth* **2013**, *364*, 16.
[27] V. Demontis, M. Rocci, M. Donarelli, R. Maiti, V. Zannier, F. Beltram, L. Sorba, S. Roddaro, F. Rossella, C. Baratto, *Sensors* **2019**, *19*, 2994.
[28] Y. Ye, Y. Dai, L. Dai, Z. Shi, N. Liu, F. Wang, L. Fu, R. Peng, X. Wen, Z. Chen, Z. Liu, G. Qin, *ACS Appl. Mater. Interfaces* **2010**, *2*, 3406.
[29] Y. Pei, R. Pei, X. Liang, Y. Wang, L. Liu, H. Chen, J. Liang, *Sci. Rep.* **2016**, *6*, 21551.
[30] H. Sumikura, G. Zhang, M. Takiguchi, N. Takemura, A. Shinya, H. Gotoh, M. Notomi, *Nano Lett.* **2019**, *19*, 8059.
[31] R. Yu, X. Wang, W. Peng, W. Wu, Y. Ding, S. Li, Z. L. Wang, *ACS Nano* **2015**, *9*, 9822.
[32] H. Chen, N. Xi, K. W. Lai, C. K. Fung, R. Yang, *IEEE Trans. Nanotechnol.* **2010**, *9*, 582.
[33] P. Krogstrup, N. L. Ziino, W. Chang, S. M. Albrecht, M. H. Madsen, E. Johnson, J. Nygard, C. M. Marcus, T. S. Jespersen, *Nat. Mater.* **2015**, *14*, 400.
[34] Y. Hu, J. Zhou, P.-H. Yeh, Z. Li, T.-Y. Wei, Z. L. Wang, *Adv. Mater.* **2010**, *22*, 3327.
[35] S. M. Sze, K. K. Ng, *Physics of Semiconductor Devices*, Wiley, New York **1981**.
[36] A. Zhang, C. M. Lieber, *Chem. Rev.* **2016**, *116*, 215.
[37] D. Nozaki, J. Kunstmann, F. Zorgiebel, W. M. Weber, T. Mikolajick, G. Cuniberti, *Nanotechnology* **2011**, *22*, 325703.
[38] F. M. Zörgiebel, S. Pregl, L. Römhildt, J. Opitz, W. Weber, T. Mikolajick, L. Baraban, G. Cuniberti, *Nano Res.* **2014**, *7*, 263.
[39] S. Carrara, D. Sacchetto, M.-A. Doucey, C. Baj-Rossi, G. De Micheli, Y. Leblebici, *Sens. Actuators, B* **2012**, *171–172*, 449.
[40] R. J. Chen, H. C. Choi, S. Bangsaruntip, E. Yenilmez, X. Tang, Q. Wang, Y.-L. Chang, H. Dai, *J. Am. Chem. Soc.* **2004**, *126*, 1563.
[41] P. H. Yeh, Z. Li, Z. L. Wang, *Adv. Mater.* **2009**, *21*, 4975.
[42] L. Zhao, H. Li, J. Meng, A. C. Wang, P. Tan, Y. Zou, Z. Yuan, J. Lu, C. Pan, Y. Fan, Y. Zhang, Y. Zhang, Z. L. Wang, Z. Li, *Adv. Funct. Mater.* **2020**, *30*, 1907999.
[43] Z. L. Wang, J. Song, *Science* **2006**, *312*, 242.
[44] C. Pan, R. Yu, S. Niu, G. Zhu, Z. L. Wang, *ACS Nano* **2013**, *7*, 1803.
[45] R. Yu, C. Pan, Z. L. Wang, *Energy Environ. Sci.* **2013**, *6*, 494.
[46] X. Cao, X. Cao, H. Guo, T. Li, Y. Jie, N. Wang, Z. L. Wang, *ACS Nano* **2016**, *10*, 8038.
[47] R. Yu, C. Pan, J. Chen, G. Zhu, Z. L. Wang, *Adv. Funct. Mater.* **2013**, *23*, 5868.
[48] L. Zhu, W. Zeng, *Sens. Actuators, A* **2017**, *267*, 242.
[49] T. Seiyama, A. Kato, K. Fujiishi, M. Nagatani, *Anal. Chem.* **1962**, *34*, 1502.
[50] M. Kumar, V. Singh Bhati, S. Ranwa, J. Singh, M. Kumar, *Sci. Rep.* **2017**, *7*, 236.
[51] T.-Y. Wei, P.-H. Yeh, S.-Y. Lu, Z. L. Wang, *J. Am. Chem. Soc.* **2009**, *131*, 17690.
[52] J. Suehiro, H. Imakiire, S.-I. Hidaka, W. Ding, G. Zhou, K. Imasaka, M. Hara, *Sens. Actuators, B* **2006**, *114*, 943.
[53] A. Zhong, T. Sasaki, K. Hane, *Sens. Actuators, A* **2014**, *209*, 52.
[54] S. M. Niu, Y. F. Hu, X. M. Wen, Y. S. Zhou, F. Zhang, L. Lin, S. H. Wang, Z. L. Wang, *Adv. Mater.* **2013**, *25*, 3701.
[55] L. Guo, Z. Yang, X. Dou, *Adv. Mater.* **2017**, *29*, 1604528.
[56] N. S. Ramgir, P. K. Sharma, N. Datta, M. Kaur, A. K. Debnath, D. K. Aswal, S. K. Gupta, *Sens. Actuators, B* **2013**, *186*, 718.
[57] N. Zhang, X. Ma, S. Ruan, Y. Yin, C. Li, H. Zhang, Y. Chen, *J. Nanosci. Nanotechnol.* **2019**, *19*, 7083.
[58] Y. Hu, Y. Chang, P. Fei, R. L. Snyder, Z. L. Wang, *ACS Nano* **2010**, *4*, 1234.
[59] Z. Yang, X. Dou, S. Zhang, L. Guo, B. Zu, Z. Wu, H. Zeng, *Adv. Funct. Mater.* **2015**, *25*, 4039.
[60] M. E. Franke, T. J. Koplin, U. Simon, *Small* **2006**, *2*, 36.
[61] W. Göpel, K. D. Schierbaum, *Sens. Actuators, B* **1995**, *26*, 1.
[62] N. Yamazoe, G. Sakai, K. Shimanoe, *Catal. Surv. Asia* **2003**, *7*, 63.
[63] W.-C. Wang, C.-Y. Lai, Y.-T. Lin, T.-H. Yua, Z.-Y. Chen, W.-W. Wu, P.-H. Yeh, *RSC Adv.* **2016**, *6*, 65146.
[64] L. Q. Zhang, Z. F. Gao, C. Liu, Y. H. Zhang, Z. Q. Tu, X. P. Yang, F. Yang, Z. Wen, L. P. Zhu, R. Liu, Y. F. Li, L. S. Cui, *J. Mater. Chem. A* **2015**, *3*, 2794.
[65] Z. Y. Zhang, Z. Wen, Z. Z. Ye, L. P. Zhu, *RSC Adv.* **2015**, *5*, 59976.
[66] Z. Y. Zhang, L. P. Zhu, Z. Wen, Z. Z. Ye, *Sens. Actuators, B* **2017**, *238*, 1052.
[67] J. Gao, L. Wang, K. Kan, S. Xu, L. Jing, S. Liu, P. Shen, L. Li, K. Shi, *J. Mater. Chem. A* **2014**, *2*, 949.
[68] X. Zhou, Y. Xiao, M. Wang, P. Sun, F. Liu, X. Liang, X. Li, G. Lu, *ACS Appl. Mater. Interfaces* **2015**, *7*, 8743.
[69] D. R. Miller, S. A. Akbar, P. A. Morris, *Sens. Actuators, B* **2014**, *204*, 250.
[70] Z.-Y. Zhao, M.-H. Wang, T.-T. Liu, *Mater. Lett.* **2015**, *158*, 274.
[71] K. Shingange, Z. P. Tshabalala, O. M. Ntwaeaborwa, D. E. Motaung, G. H. Mhlongo, *J. Colloid Interface Sci.* **2016**, *479*, 127.
[72] F.-C. Chung, Z. Zhu, P.-Y. Luo, R.-J. Wu, W. Li, *Sens. Actuators, B* **2014**, *199*, 314.
[73] N. S. Ramgir, P. K. Sharma, N. Datta, M. Kaur, A. K. Debnath, D. K. Aswal, S. K. Gupta, *Sens. Actuators, B* **2013**, *186*, 718.
[74] D.-T. Phan, G.-S. Chung, *J. Electroceram.* **2014**, *32*, 353.
[75] S.-C. Wang, M. O. Shaikh, *Sensors* **2015**, *15*, 14286.
[76] Y. Wang, B. Liu, D. Cai, H. Li, Y. Liu, D. Wang, L. Wang, Q. Li, T. Wang, *Sens. Actuators, B* **2014**, *201*, 351.
[77] J. M. Lee, J.-E. Park, S. Kim, S. Kim, E. Lee, S.-J. Kim, W. Lee, *Int. J. Hydrogen Energy* **2010**, *35*, 12568.
[78] H.-Y. Lai, C.-H. Chen, *J. Mater. Chem.* **2012**, *22*, 13204.
[79] P. Patil, G. Gaikwad, D. Patil, J. Naik, *Bull. Mater. Sci.* **2016**, *39*, 655.
[80] J. Wang, X. Li, Y. Xia, S. Komarneni, H. Chen, J. Xu, L. Xiang, D. Xie, *ACS Appl. Mater. Interfaces* **2016**, *8*, 8600.
[81] R. K. Sonker, B. Yadav, A. Sharma, M. Tomar, V. Gupta, *RSC Adv.* **2016**, *6*, 56149.
[82] K. Dunst, J. Karczewski, P. Jasiński, *Sens. Actuators, B* **2017**, *247*, 108.
[83] A. Gusain, N. J. Joshi, P. Varde, D. Aswal, *Sens. Actuators, B* **2017**, *239*, 734.
[84] J. Iqbal, T. Jan, Y. Ronghai, *J. Mater. Sci.: Mater. Electron.* **2013**, *24*, 4393.
[85] G. K. Mani, J. B. B. Rayappan, *J. Alloys Compd.* **2014**, *582*, 414.
[86] G. K. Mani, J. B. B. Rayappan, *Sens. Actuators, B* **2016**, *223*, 343.
[87] J. Cui, J. Jiang, L. Shi, F. Zhao, D. Wang, Y. Lin, T. Xie, *RSC Adv.* **2016**, *6*, 78257.
[88] M. Stoppa, A. Chiolerio, *Sensors* **2014**, *14*, 11957.
[89] L. Cai, C. Wang, *Nanoscale Res. Lett.* **2015**, *10*, 320.
[90] Q. Zheng, J. Huang, S. Cao, H. Gao, *J. Mater. Chem. C* **2015**, *3*, 7469.
[91] B. Nie, J. G. Hu, L. B. Luo, C. Xie, L. H. Zeng, P. Lv, F. Z. Li, J. S. Jie, M. Feng, C. Y. Wu, *Small* **2013**, *9*, 2872.
[92] T. F. Zhang, Z. P. Li, J. Z. Wang, W. Y. Kong, G. A. Wu, Y. Z. Zheng, Y. W. Zhao, E. X. Yao, N. X. Zhuang, L. B. Luo, *Sci. Rep.* **2016**, *6*, 38569.
[93] T.-Y. Wei, C.-T. Huang, B. J. Hansen, Y.-F. Lin, L.-J. Chen, S.-Y. Lu, Z. L. Wang, *Appl. Phys. Lett.* **2010**, *96*, 013508.
[94] J. Zhou, Y. Gu, Y. Hu, W. Mai, P.-H. Yeh, G. Bao, A. K. Sood, D. L. Polla, Z. L. Wang, *Appl. Phys. Lett.* **2009**, *94*, 191103.

[95] X. Zhang, B. Liu, Q. Liu, W. Yang, C. Xiong, J. Li, X. Jiang, *ACS Appl. Mater. Interfaces* **2017**, *9*, 2669.
[96] N. Han, Z. X. Yang, F. Wang, G. Dong, S. Yip, X. Liang, T. F. Hung, Y. Chen, J. C. Ho, *ACS Appl. Mater. Interfaces* **2015**, *7*, 20454.
[97] Y. Luo, X. Yan, J. Zhang, B. Li, Y. Wu, Q. Lu, C. Jin, X. Zhang, X. Ren, *Nanoscale* **2018**, *10*, 9212.
[98] J. Miao, W. Hu, N. Guo, Z. Lu, X. Liu, L. Liao, P. Chen, T. Jiang, S. Wu, J. C. Ho, L. Wang, X. Chen, W. Lu, *Small* **2015**, *11*, 936.
[99] S. Lu, J. Qi, S. Liu, Z. Zhang, Z. Wang, P. Lin, Q. Liao, Q. Liang, Y. Zhang, *ACS Appl. Mater. Interfaces* **2014**, *6*, 14116.
[100] Q. Yang, X. Guo, W. Wang, Y. Zhang, S. Xu, D. H. Lien, Z. L. Wang, *ACS Nano* **2010**, *4*, 6285.
[101] X. Q. Shi, M. Z. Peng, J. Z. Kou, C. H. Liu, R. Wang, Y. D. Liu, J. Y. Zhai, *Adv. Electron. Mater.* **2015**, *1*, 1500169.
[102] X. Han, W. Du, R. Yu, C. Pan, Z. L. Wang, *Adv. Mater.* **2015**, *27*, 7963.
[103] Y. Wang, L. Zhu, Y. Feng, Z. Wang, Z. L. Wang, *Adv. Funct. Mater.* **2019**, *29*, 1807111.
[104] W. B. Peng, X. F. Wang, R. M. Yu, Y. J. Dai, H. Y. Zou, A. C. Wang, Y. N. He, Z. L. Wang, *Adv. Mater.* **2017**, *29*, 1606698.
[105] Z. N. Wang, R. M. Yu, X. F. Wang, W. Z. Wu, Z. L. Wang, *Adv. Mater.* **2016**, *28*, 6880.
[106] W. B. Peng, R. M. Yu, X. F. Wang, Z. N. Wang, H. Y. Zou, Y. N. He, Z. L. Wang, *Nano Res.* **2016**, *9*, 3695.
[107] N. Ma, K. W. Zhang, Y. Yang, *Adv. Mater.* **2017**, *29*, 1703694.
[108] N. Ma, Y. Yang, *Nano Energy* **2017**, *40*, 352.
[109] D. You, C. Xu, W. Zhang, J. Zhao, F. Qin, Z. Shi, *Nano Energy* **2019**, *62*, 310.
[110] Z. N. Wang, R. M. Yu, C. F. Pan, Z. L. Li, J. Yang, F. Yi, Z. L. Wang, *Nat. Commun.* **2015**, *6*, 8401.
[111] X. Liu, L. Gu, Q. Zhang, J. Wu, Y. Long, Z. Fan, *Nat. Commun.* **2014**, *5*, 4007.
[112] X. L. Zhang, Q. Y. Liu, B. D. Liu, W. J. Yang, J. Li, P. J. Niu, X. Jiang, *J. Mater. Chem. C* **2017**, *5*, 4319.
[113] X. Zhao, F. Wang, L. Shi, Y. Wang, H. Zhao, D. Zhao, *RSC Adv.* **2016**, *6*, 4634.
[114] H. X. Li, X. H. Zhang, N. S. Liu, L. W. Ding, J. Y. Tao, S. L. Wang, J. Su, L. Y. Li, Y. H. Gao, *Opt. Express* **2015**, *23*, 21204.
[115] J. Zhou, Y. Gu, P. Fei, W. Mai, Y. Gao, R. Yang, G. Bao, Z. L. Wang, *Nano Lett.* **2008**, *8*, 3035.
[116] W. G. Zhang, R. Zhu, V. Nguyen, R. S. Yang, *Sens. Actuators, A* **2014**, *205*, 164.
[117] J. M. Wu, C. Y. Chen, Y. Zhang, K. H. Chen, Y. Yang, Y. F. Hu, J. H. He, Z. L. Wang, *ACS Nano* **2012**, *6*, 4369.
[118] Z. Zhang, Q. L. Liao, X. H. Zhang, G. J. Zhang, P. F. Li, S. N. Lu, S. Liu, Y. Zhang, *Nanoscale* **2015**, *7*, 1796.
[119] Q. L. Liao, M. Mohr, X. H. Zhang, Z. Zhang, Y. Zhang, H. J. Fecht, *Nanoscale* **2013**, *5*, 12350.
[120] Y. Yang, J. J. Qi, Y. S. Gu, X. Q. Wang, Y. Zhang, *Phys. Status Solidi RRL* **2009**, *3*, 269.
[121] W. J. Mai, Z. W. Liang, L. Zhang, X. Yu, P. Y. Liu, H. M. Zhu, X. Cai, S. Z. Tan, *Chem. Phys. Lett.* **2012**, *538*, 99.
[122] Y. Yang, W. Guo, J. J. Qi, J. Zhao, Y. Zhang, *Appl. Phys. Lett.* **2010**, *97*, 223113.
[123] Y. Chang, D. Hasan, B. Dong, J. Wei, Y. Ma, G. Zhou, K. W. Ang, C. Lee, *ACS Appl. Mater. Interfaces* **2018**, *10*, 38272.
[124] D. Hasan, C. Lee, *Adv. Sci.* **2018**, *5*, 1700581.
[125] Z. Ren, Y. Chang, Y. Ma, K. Shih, B. Dong, C. Lee, *Adv. Opt. Mater.* **2020**, *8*, 1900653.
[126] W. Z. Wu, C. F. Pan, Y. Zhang, X. N. Wen, Z. L. Wang, *Nano Today* **2013**, *8*, 619.
[127] Z. L. Wang, W. Z. Wu, *Natl. Sci. Rev.* **2014**, *1*, 62.
[128] Y. Zhang, Y. Liu, Z. L. Wang, *Adv. Mater.* **2011**, *23*, 3004.
[129] W. Liu, A. Zhang, Y. Zhang, Z. L. Wang, *Nano Energy* **2015**, *14*, 355.
[130] Z. L. Wang, *J. Phys. Chem. Lett.* **2010**, *1*, 1388.
[131] C. Pan, J. Zhai, Z. L. Wang, *Chem. Rev.* **2019**, *119*, 9303.
[132] Y. Hu, Y. Chang, P. Fei, R. L. Snyder, Z. L. Wang, *ACS Nano* **2010**, *4*, 1234.
[133] J. M. Shannon, *Solid-State Electron.* **1976**, *19*, 537.
[134] F. Xue, L. M. Zhang, X. L. Feng, G. F. Hu, F. R. Fan, X. N. Wen, L. Zheng, Z. L. Wang, *Nano Res.* **2015**, *8*, 2390.
[135] Y. Ding, Y. Liu, S. M. Niu, W. Z. Wu, Z. L. Wang, *J. Appl. Phys.* **2014**, *116*, 154304.
[136] F. Zhang, Y. Ding, Y. Zhang, X. Zhang, Z. L. Wang, *ACS Nano* **2012**, *6*, 9229.
[137] J. Zhang, X. Liu, G. Neri, N. Pinna, *Adv. Mater.* **2016**, *28*, 795.
[138] A. Gurlo, R. Riedel, *Angew. Chem., Int. Ed.* **2007**, *46*, 3826.
[139] X. Y. Xue, L. L. Xing, Y. J. Chen, S. L. Shi, Y. G. Wang, T. H. Wang, *J. Phys. Chem. C* **2008**, *112*, 12157.
[140] D. Guo, Q. Guo, Z. Chen, Z. Wu, P. Li, W. Tang, *Mater. Today Phys.* **2019**, *11*, 100157.
[141] Z. Liu, Q. Zheng, Y. Shi, L. Xu, Y. Zou, D. Jiang, B. Shi, X. Qu, H. Li, H. Ouyang, R. Liu, Y. Wu, Y. Fan, Z. Li, *J. Mater. Chem. B* **2020**.
[142] C. Wang, K. Hu, C. Zhao, Y. Zou, Y. Liu, X. Qu, D. Jiang, Z. Li, M.-R. Zhang, Z. Li, *Small* **2020**, *16*, 1904758.
[143] Z. L. Wang, *ACS Nano* **2013**, *7*, 9533.
[144] Y. Zou, P. Tan, B. Shi, H. Ouyang, D. Jiang, Z. Liu, H. Li, M. Yu, C. Wang, X. Qu, L. Zhao, Y. Fan, Z. L. Wang, Z. Li, *Nat. Commun.* **2019**, *10*, 2695.
[145] Z. Liu, Y. Ma, H. Ouyang, B. Shi, N. Li, D. Jiang, F. Xie, D. Qu, Y. Zou, Y. Huang, *Adv. Funct. Mater.* **2019**, *29*, 1807560.
[146] J. Sun, A. Yang, C. Zhao, F. Liu, Z. Li, *Sci. Bull.* **2019**, *64*, 1336.
[147] B. Shi, Z. Liu, Q. Zheng, J. Meng, H. Ouyang, Y. Zou, D. Jiang, X. Qu, M. Yu, L. Zhao, Y. Fan, Z. L. Wang, Z. Li, *ACS Nano* **2019**, *13*, 6017.
[148] X. Q. Zhang, M. Yu, Z. R. Ma, H. Ouyang, Y. Zou, S. L. Zhang, H. K. Niu, X. X. Pan, M. Y. Xu, Z. Li, Z. L. Wang, *Adv. Funct. Mater.* **2019**, *29*, 1900327.